Acta Mech 226, 625–642 (2015)
DOI 10.1007/s00707-014-1192-3

J. L. Mantari · C. Guedes Soares

A quasi-3D tangential shear deformation theory with four unknowns for functionally graded plates

Received: 5 December 2013 / Revised: 8 June 2014 / Published online: 25 July 2014

Abstract A so far unavailable quasi-3D trigonometric shear deformation theory for the bending analysis of functionally graded plates is presented. This theory considers the thickness-stretching effect ($\varepsilon_{zz} \neq 0$) by modeling the displacement field with just four unknowns and rich trigonometric shear strain shape functions. The principle of virtual works is used to derive the governing equations and boundary conditions. Results from this theory are compared with the CPT, first-order shear deformation theory (FSDT), and other quasi-3D HSDTs. In conclusion, this theory is more accurate than the CPT and FSDT and behaves as well as quasi-3D HSDTs having much less number of unknowns.

1 Introduction

The concept of functionally graded materials (FGMs) is not new [1,2]. This kind of material can be found in nature. FGMs are found in sea shells and bones, and the understanding of the high complexity of such materials is contributing to the synthesizing of new kinds of materials. Currently, FGMs are alternative materials widely used in the industry [3].

Mechanically, FGMs are both macroscopically and microscopically heterogeneous materials, which are normally made, for example, from a mixture of ceramics and metals with continuous composition gradation from pure ceramic on one surface to full metal on the other. Such gradation leads to smooth change in the material profile as well as the effective physical properties to overcome the usual problems when classical laminate composites are used.

Functionally graded materials (FGMs) can be used to build any kind of structures such as shells. For example, representative research on the static response of functionally graded plates (FGPs) is available in the literature, see, for example, the works by Jha et al. [3] and Birman and Byrd [4]. This paper deals with the development of a shear deformation theory that is applied to study the bending response of FGPs, and therefore, a review on the developments of theories for FGMs is described in the following.

Usually, when a shear deformation theory is developed, one can use either displacement-based theories (when the principle of virtual displacement is used), stress-based theories, or displacement–stress-based theories (when Reissner mixed variational theorem is used), see [5–13] for details. The well-described Carrera's unified formulation (CUF) [14], which is extended by Demasi [5,6,10–13] in the so-called generalized unified formulation (GUF), describes precisely and clearly the models, types, and classes of theories.

J. L. Mantari · C. Guedes Soares (✉)
Centre for Marine Technology and Engineering (CENTEC), Instituto Superior Técnico,
Universidade de Lisboa, Av. Rovisco Pais, 1049-001 Lisbon, Portugal
E-mail: c.guedes.soares@centec.tecnico.ulisboa.pt
Tel.: +351 218 417607
URL: http://www.mar.ist.utl.pt/

In the context of shear deformation theories, a significant number of theories for plates and shells have been developed in the last and in the beginning of this century. These theories can be classified into different models, such as equivalent single layer, quasi-layerwise, and layerwise models [5,6]. Within them, as is well known, there are mainly three major theories, namely the classical lamination theory (CLT), which is based on the assumptions of Kirchhoff's plate theory that neglects the interlaminar shear deformation; the first-order shear deformation theory (FSDT), which assumes constant transverse shear deformation through the entire thickness of the laminate and violates stress-free boundary conditions at the top and bottom surfaces of the plate; and more accurate theories such as higher-order theories (HSDTs) assuming quadratic, cubic, or non-polynomial variations of surface-parallel displacements through the entire thickness of the laminates to model the behavior of the structure for thick-to-thin regions.

The above-mentioned theories were applied to isotropic, classical, and advanced composite beams, plates, and shells. The present paper will only consider the contributions on advanced composite structures such as FGPs. In this context, in the last decade, several researchers investigated the static and dynamic behavior of FGMs. For example, Reddy [15] presented Navier's solutions and finite element models including geometric nonlinearity based on the third-order shear deformation theory for the analysis of FGPs. Cheng and Batra [16] derived the field equations for a FGP using both FSDT and HSDT. Kashtalyan [17] presented a three-dimensional elasticity solution for a functionally graded simply supported plate under transversely distributed load.

Ferreira et al. [18] used a meshless method for the static analysis of a simply supported FGP by a polynomial HSDT. Elishakoff [19] developed a three-dimensional elasticity solution using the Ritz method for the static response of a clamped rectangular FGP. The static response of FGPs was presented by Zenkour [20] using the generalized shear deformation theory developed by the author. Ramirez et al. [21] developed a discrete layer model in conjunction with the Ritz method for the approximate solution of a static analysis for the two types of FGPs.

Zenkour [22] investigated the static problem of transverse load acting on exponentially graded (EG) rectangular plates using both 2D trigonometric plate theory (TPT) and 3D elasticity solution. The quasi-3D HSDT presented in this paper includes the thickness-stretching effect. Sladek et al. [23] presented the static and dynamic analysis of FGPs by the meshless local Petrov–Galerkin method. The Reissner–Mindlin assumptions were utilized to describe the plate deformation. Numerical results were presented for simply supported and clamped plates. In Sladek et al. [24,25], the authors applied the same method to solve plates and shell problems under thermal loading.

Abrate [26] deduced, by using the CPT, that no special tools are required to analyze FGPs, because an FGP behaves like homogeneous plates. Bo et al. [27] presented the elasticity solutions for the static analysis of FGPs for different boundary conditions. Stress, free vibration, and buckling analysis due to mechanical and thermal loads were given by Matsunaga [28–30] by using a kind of generalized two-dimensional HSDT. This interesting theory was obtained by using the method of power series expansion of continuous displacement components.

Khabbaz et al. [31] provided a nonlinear solution of FGM plates using the first- and third-order shear deformation theories. Aghdam et al. [32] presented a static analysis of fully clamped FGPs and doubly curved panels by using the extended Kantorovich method. Zenkour and Alghamdi [33], using a variety of equivalent single-layer theories (ESLTs), studied the thermo-bending problems of FG sandwich plates, consisting of a homogeneous core layer bounded with two FGM face-sheet layers, in which the material properties of the face-sheet layers were assumed to obey a power-law distribution of the volume fractions of the constituents through the thickness coordinate. Wu and Li [34] used a RMVT-based and HSDT to study the response of multilayered FGPs under mechanical loads.

Talha and Singh [35] investigated the free vibration and static analysis of FGPs using a non-conforming finite element formulation by employing a quasi-3D polynomial HSDT. Vaghefi et al. [36] presented a three-dimensional static solution for thick FGPs by utilizing a meshless Petrov–Galerkin method. RMVT-based meshless collocation and element-free Galerkin methods for the quasi-3D analysis of multilayered composite and FGM plates and circular hollow cylinders were presented by Wu et al. [37] and Wu and Yang [38].

Benachour et al. [39] developed a four-unknown HSDT without including the thickness-stretching effect for free vibration analysis of plates made of FGMs with an arbitrary gradient. Thai and Choi [40] studied the free vibration analysis of FG plates on elastic foundation by using similar refined plate theory as the one presented in [39]. Reddy and Kim [41] proposed a general nonlinear third-order plate theory that accounts for geometric nonlinearity, microstructure-dependent size effects, and two-constituent material variation through the plate thickness using the principle of virtual displacements and Hamilton's principle.

In Carrera et al. [42], the influence of the thickness-stretching effect on the bending responses of FGPs and shells was investigated in the context of Carreras's unified formulation (CUF). In fact, this work is an extension of several FGM papers published by using CUF [43–46]. Based on the previous experience on meshless numerical method, Neves et al. [47–50] and Ferreira et al. [51] powered CUF in a remarkable joint work between the authors.

In Mantari et al. [52,53] and Mantari and Guedes Soares [54], bending results of FG plates by using new non-polynomial HSDTs were presented. The authors used five-unknown HSDTs without including the thickness-stretching effect. In [55] and [56], the thickness-stretching effect was included by adding one unknown in the displacement field (six-unknown HSDTs), and improved results of displacements and in-plane normal stresses compared with [52] and [53] were obtained.

Xiang et al. [57] developed an *n*th-order HSDT for advanced composite plates with similar fashion as the one developed by Matsunaga [28–30]. The authors realize that the polynomial HSDT with order 3 predicts good results corroborating in this way the HSDT proposed by Reddy [15]. Mechab et al. [58] considered the static and dynamic analysis of FGPs by using the four-unknown HSDTs ($\varepsilon_{zz} = 0$) and non-polynomial shear strain shape function. Thai and Kim [59] developed a five-unknown TPT with thickness-stretching effect with good accuracy with respect to its counterpart, the TPT with six unknowns. Mantari and Guedes Soares [60,61] developed an optimized TPT with stretching effect (five and six unknowns) with improved results compared with the five- and six-unknown quasi-3D trigonometric plate theories [22,59]. Recently, Zenkour [62] developed an interesting HSDT with four unknowns and thickness-stretching effect, different to the one proposed in this paper.

In this paper, a new trigonometric quasi-3D HSDT with four unknowns and thickness-stretching effect is presented. The beauty of this theory is that, in addition to including the thickness-stretching effect ($\varepsilon_{zz} \neq 0$), the displacement field is modeled with only four unknowns, which is even less than in the FSDT and does not need a shear correction factor. The principle of virtual works is used to derive the governing equations and boundary conditions. Analytical results from the new theory are compared with the CPT, FSDT, and other quasi-3D HSDTs. In conclusion, this theory is more accurate than the CPT and FSDT and behaves as well as quasi-3D HSDTs having a much smaller number of unknowns. Therefore, trade-offs between computational cost and accuracy of the present theory should be further studied.

2 Theoretical formulation

An FGP of uniform thickness h is shown in Fig. 1. Both an exponentially graded plate (EGP) and a powerly graded plate (PGP) are shown. The displacement field satisfying the conditions of transverse shear stresses (and hence strains) vanishing at a point $(x,\ y,\ \pm h/2)$ on the outer (top) and inner (bottom) surfaces of the plate is given as follows:

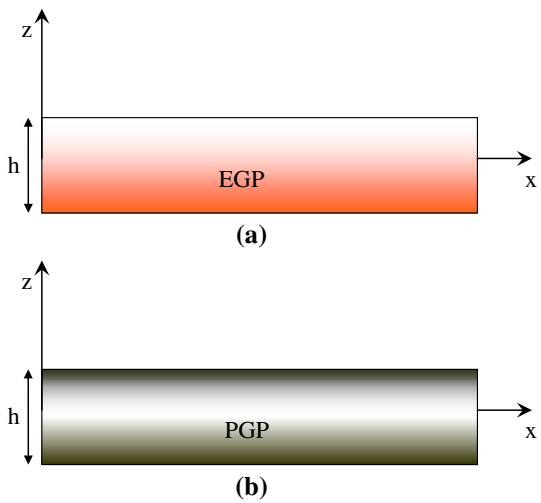

Fig. 1 Geometry of a functionally graded plate

$$\begin{aligned}
\overline{u} &= u + z\left[y^{**}\frac{\partial w_b}{\partial x} + q^{**}\frac{\partial w_s}{\partial x}\right] + f(z)\frac{\partial w_s}{\partial x},\\
\overline{v} &= v + z\left[y^{**}\frac{\partial w_b}{\partial y} + q^{**}\frac{\partial w_s}{\partial y}\right] + f(z)\frac{\partial w_s}{\partial y},\\
\overline{w} &= w_b + g(z)w_s,
\end{aligned} \tag{1a–c}$$

where $u(x, y)$, $v(x, y)$, $w_b(x, y)$, and $w_s(x, y)$ are the four unknown displacement functions of the middle surface of the panel, $f(z) = \frac{h}{m}\tan\left(\frac{mz}{h}\right) + z^3$, $g(z) = nf'(z)$, while $y^{**} = -1$, $y^* = -f'\left(\frac{h}{2}\right)$, $q^* = -g\left(\frac{h}{2}\right)$ and $q^{**} = y^* + q^*$ (being h the thickness of the plate, see Fig. 1 for more details). The shape strain functions are expressed in such way by considering basic ideas from Zenkour [62] and Mantari and Guedes Soares [55]. In Eqs. (1a–c), the displacement field includes the parameters m and n into the shear strain shape functions. These parameters are selected in Sect. 4 with the idea to obtain close to 3D results.

The starting point of the present thick plate theory is the 3D elasticity theory [63]. In the derivation of the necessary equations, small elastic deformations are assumed, i.e., displacements and rotations are small, and obey Hooke's law. The strain–displacement relations, based on this formulation, are written as follows:

$$\begin{aligned}
\varepsilon_{xx} &= \varepsilon^0_{xx} + z\varepsilon^1_{xx} + f(z)\varepsilon^2_{xx},\\
\varepsilon_{yy} &= \varepsilon^0_{yy} + z\varepsilon^1_{yy} + f(z)\varepsilon^2_{yy},\\
\varepsilon_{zz} &= g'(z)\varepsilon^5_{zz},\\
\varepsilon_{yz} &= \varepsilon^0_{yz} + g(z)\varepsilon^3_{yz} + f'(z)\varepsilon^4_{yz},\\
\varepsilon_{xz} &= \varepsilon^0_{xz} + g(z)\varepsilon^3_{xz} + f'(z)\varepsilon^4_{xz},\\
\varepsilon_{xy} &= \varepsilon^0_{xy} + z\varepsilon^1_{xy} + f(z)\varepsilon^2_{xy},
\end{aligned} \tag{2a–f}$$

where

$$\begin{aligned}
&\varepsilon^0_{xx} = \frac{\partial u}{\partial x}, \quad \varepsilon^1_{xx} = y^{**}\frac{\partial^2 w_b}{\partial x^2} + q^{**}\frac{\partial^2 w_s}{\partial x^2}, \quad \varepsilon^2_{xx} = \frac{\partial^2 w_s}{\partial x^2},\\
&\varepsilon^0_{yy} = \frac{\partial v}{\partial y}, \quad \varepsilon^1_{yy} = y^{**}\frac{\partial^2 w_b}{\partial y^2} + q^{**}\frac{\partial^2 w_s}{\partial y^2}, \quad \varepsilon^2_{yy} = \frac{\partial^2 w_s}{\partial y^2},\\
&\varepsilon^5_{zz} = w_s,\\
&\varepsilon^0_{yz} = q^{**}\frac{\partial w_s}{\partial y}, \quad \varepsilon^3_{yz} = \frac{\partial w_s}{\partial y}, \quad \varepsilon^4_{yz} = \frac{\partial w_s}{\partial y}\\
&\varepsilon^0_{xz} = q^{*}\frac{\partial w_s}{\partial x}, \quad \varepsilon^3_{xz} = \frac{\partial w_s}{\partial x}, \quad \varepsilon^4_{xz} = \frac{\partial w_s}{\partial x}\\
&\varepsilon^0_{xy} = \frac{\partial v}{\partial x} + \frac{\partial u}{\partial y}, \quad \varepsilon^1_{xy} = 2y^{**}\frac{\partial^2 w_b}{\partial x\partial y} + 2q^{**}\frac{\partial^2 w_s}{\partial x\partial y}, \quad \varepsilon^2_{xy} = 2\frac{\partial^2 w_s}{\partial x\partial y}.
\end{aligned} \tag{3a–p}$$

An FGP of length a, width b, and a total thickness h made of a mixture of metal and ceramic materials are considered in the present analysis. The effective material properties of the FGPs, $\mathbf{P}_{(z)}$, vary through the plate thickness according to the function $V_{(z)}$ as shown in the following equation:

$$P(z) = \begin{cases} V_{(z)}P_b, & V_{(z)} = e^{p\left(\frac{z}{h}+\frac{1}{2}\right)}, \quad \text{Case 1 (exponentially graded)},\\ (P_t - P_b)V_{(z)} + P_b, & V_{(z)} = \left(\frac{z}{h}+\frac{1}{2}\right)^p, \quad \text{Case 2 (powerly graded)}, \end{cases} \tag{4a–b}$$

where P_t and P_b denote the property of the top and bottom faces of the panel, respectively, and p is the exponent that specifies the material variation profile through the thickness. In this paper, for example, the Young's modulus, E, and shear modulus, G, vary depending on the case problem according to Eqs. (4a–b), and the Poisson ratio, ν is assumed to be constant.

Figure 2 shows the exponential function $V(z)$ along the thickness of an EGP for different values of the parameter p, while Fig. 3 shows the corresponding function for a PGP.

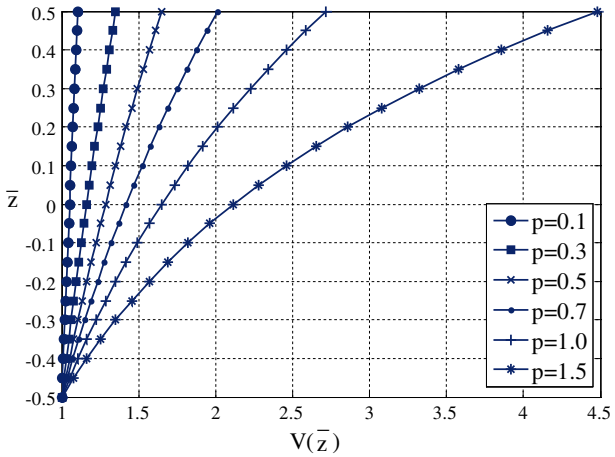

Fig. 2 Exponentially graded function $V(\bar{z})$ along the thickness of an EGP for different values of the parameter p

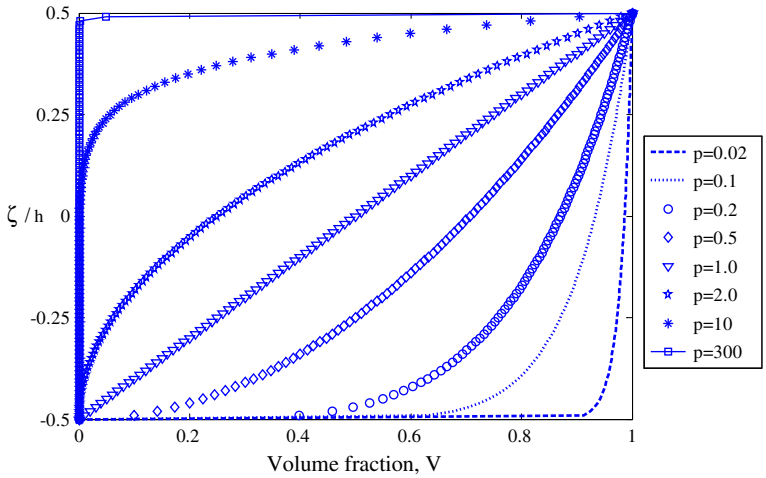

Fig. 3 Powerly graded function $V(\bar{z})$ along the thickness of an PGP for different values of the parameter p

The linear constitutive relations are given by:

$$\begin{Bmatrix} \sigma_{xx} \\ \sigma_{yy} \\ \sigma_{zz} \\ \tau_{yz} \\ \tau_{xz} \\ \tau_{xy} \end{Bmatrix}^{k}_{(z)} = \begin{bmatrix} Q_{11} & Q_{12} & Q_{13} & 0 & 0 & 0 \\ Q_{21} & Q_{22} & Q_{23} & 0 & 0 & 0 \\ Q_{31} & Q_{32} & Q_{33} & 0 & 0 & 0 \\ 0 & 0 & 0 & Q_{44} & 0 & 0 \\ 0 & 0 & 0 & 0 & Q_{55} & \\ 0 & 0 & 0 & 0 & 0 & Q_{66} \end{bmatrix}^{k}_{(z)} \begin{Bmatrix} \varepsilon_{xx} \\ \varepsilon_{yy} \\ \varepsilon_{zz} \\ \gamma_{yz} \\ \gamma_{xz} \\ \gamma_{xy} \end{Bmatrix}^{k}_{(z)} \tag{5}$$

in which $\sigma^{k}_{(z)} = \{\sigma_{xx}, \sigma_{yy}, \sigma_{zz}, \tau_{yz}, \tau_{xz}, \tau_{xy}\}^{\mathrm{T}}$ and $\varepsilon^{k}_{(z)} = \{\varepsilon_{xx}, \varepsilon_{yy}, \varepsilon_{zz}, \gamma_{yz}, \gamma_{xz}, \gamma_{xy}\}^{\mathrm{T}}$ are the stresses and the strain vectors with respect to the plate coordinate system. The Q_{ij} expressions in terms of engineering constants are given by:

$$\begin{aligned} Q_{11(z)} &= Q_{22(z)} = Q_{33(z)} = \frac{E(z)(1-\upsilon)}{(1-2\upsilon)(1+\upsilon)}, \\ Q_{12(z)} &= Q_{13(z)} = Q_{23(z)} = \frac{E(z)\upsilon}{(1-2\upsilon)(1+\upsilon)}, \\ Q_{44(z)} &= Q_{55(z)} = Q_{66(z)} = \frac{E(z)}{2(1+\upsilon)}. \end{aligned} \tag{6a–c}$$

Considering the static version of the principle of virtual work, the following expressions can be obtained:

$$0 = \left[\int_{-h/2}^{h/2}\left\{\int_{\Omega}\left[\sigma_{xx}^{(k)}\delta\varepsilon_{xx}+\sigma_{yy}^{(k)}\delta\varepsilon_{yy}+\sigma_{zz}^{(k)}\delta\varepsilon_{zz}+\sigma_{yz}^{(k)}\delta\varepsilon_{yz}+\sigma_{xz}^{(k)}\delta\varepsilon_{xz}+\sigma_{xy}^{(k)}\delta\varepsilon_{xy}\right]\mathrm{d}x\mathrm{d}y\right\}\mathrm{d}z\right] - \left[\int_{\Omega} q\delta\overline{w}\mathrm{d}x\mathrm{d}y\right], \tag{7}$$

$$0 = \int_{\Omega}\Big(N_1\delta\varepsilon_{xx}^0+M_1\delta\varepsilon_{xx}^1+P_1\delta\varepsilon_{xx}^2+N_2\delta\varepsilon_{yy}^0+M_2\delta\varepsilon_{yy}^1+P_2\delta\varepsilon_{yy}^2+R_3\delta\varepsilon_{zz}^4+N_4\delta\varepsilon_{yz}^0+Q_4\delta\varepsilon_{yz}^3 + K_4\delta\varepsilon_{yz}^4+N_5\delta\varepsilon_{xz}^0+Q_5\delta\varepsilon_{xz}^3+K_5\delta\varepsilon_{xz}^4+N_6\delta\varepsilon_{xy}^0+M_6\delta\varepsilon_{xy}^1+P_6\delta\varepsilon_{xy}^2-q\delta\overline{w}\Big)\mathrm{d}x\mathrm{d}y, \tag{8}$$

where $\varepsilon^{(k)}$ and $\sigma^{(k)}$ are the stresses and the strain vectors of the kth layer; q is the distributed transverse load; and N_i, M_i, P_i, Q_i, K_i and R_i are the resultants of the following integrations:

$$\begin{aligned}
\left(N_i, M_i, P_i\right) &= \sum_{k=1}^{N}\int_{z^{(k-1)}}^{z^{(k)}}\sigma_{i(z)}^{(k)}(1, z, f(z))\mathrm{d}z \quad (i=1,2,6),\\
N_i &= \sum_{k=1}^{N}\int_{z_{(k-1)}}^{z^{(k)}}\sigma_{i(z)}^{(k)}\mathrm{d}z \quad (i=4,5),\\
(Q_i, K_i) &= \sum_{k=1}^{N}\int_{z^{(k-1)}}^{z^{(k)}}\sigma_{i(z)}^{(k)}(g(z), f'(z))\mathrm{d}z \quad (\mathrm{i}=4,5),\\
R_i &= \sum_{k=1}^{N}\int_{z^{(k-1)}}^{z^{(k)}}\sigma_{i(z)}^{(k)}g'(z)\mathrm{d}z \quad (i=3).
\end{aligned} \tag{9a–d}$$

The static version of the governing equations is derived from Eq. (8) by integrating the displacement gradients by parts and setting the coefficients of δu, δv, δw_b, and δw_s to zero separately. The generalized equations are obtained as follows:

$$\begin{aligned}
&\delta u : \frac{\partial N_1}{\partial x}+\frac{\partial N_6}{\partial y}=0,\\
&\delta v : \frac{\partial N_2}{\partial y}+\frac{\partial N_6}{\partial x}=0,\\
&\delta w_b : y^{**}\left(\frac{\partial^2 M_1}{\partial x^2}+\frac{\partial^2 M_2}{\partial y^2}+2\frac{\partial^2 M_6}{\partial x\partial y}\right)=q,\\
&\delta w_s : q^{**}\left(\frac{\partial^2 M_1}{\partial x^2}+\frac{\partial^2 M_2}{\partial y^2}+2\frac{\partial^2 M_6}{\partial x\partial y}\right)+\frac{\partial P_1}{\partial x^2}-\frac{\partial P_2}{\partial y^2}+2\frac{\partial^2 P_6}{\partial x\partial y}-q^{**}\left(\frac{\partial N_4}{\partial y}+\frac{\partial N_5}{\partial x}\right)\\
&\qquad -\left(\frac{\partial Q_4}{\partial y}+\frac{\partial Q_5}{\partial x}\right)-\left(\frac{\partial K_4}{\partial y}+\frac{\partial K_5}{\partial x}\right)=-q^{*}q.
\end{aligned} \tag{10a–d}$$

By substituting the stress–strain relations into the definitions of force and moment resultants of the present theory given in Eqs. (9a–d), the following constitutive equations are obtained:

$$\begin{aligned}
N_i &= A_{ij}\varepsilon_j^0+B_{ij}\varepsilon_j^1+C_{ij}\varepsilon_j^2+D_{ij}\varepsilon_j^3+E_{ij}\varepsilon_j^4+F_{ij}\varepsilon_j^5, \quad (i=1,2,4,5,6),\\
M_i &= B_{ij}\varepsilon_j^0+G_{ij}\varepsilon_j^1+H_{ij}\varepsilon_j^2+I_{ij}\varepsilon_j^3+J_{ij}\varepsilon_j^4+K'_{ij}\varepsilon_j^5, \quad (i=1,2,6),
\end{aligned}$$

$$
\begin{aligned}
P_i &= C_{ij}\varepsilon_j^0 + H_{ij}\varepsilon_j^1 + L_{ij}\varepsilon_j^2 + M'_{ij}\varepsilon_j^3 + N'_{ij}\varepsilon_j^4 + O_{ij}\varepsilon_j^5, \quad (i = 1, 2, 6),\\
Q_i &= D_{ij}\varepsilon_j^0 + I_{ij}\varepsilon_j^1 + M_{ij}\varepsilon_j^2 + P'_{ij}\varepsilon_j^3 + Q'_{ij}\varepsilon_j^4 + R'_{ij}\varepsilon_j^5, \quad (i = 4, 5),\\
K_i &= E_{ij}\varepsilon_j^0 + J_{ij}\varepsilon_j^1 + N'_{ij}\varepsilon_j^2 + Q'_{ij}\varepsilon_j^3 + S_{ij}\varepsilon_j^4 + T_{ij}\varepsilon_j^5, \quad (\mathrm{i} = 4, 5)\\
R_i &= F_{ij}\varepsilon_j^0 + K'_{ij}\varepsilon_j^1 + O_{ij}\varepsilon_j^2 + R'_{ij}\varepsilon_j^3 + T_{ij}\varepsilon_j^4 + U_{ij}\varepsilon_j^5, \quad (i = 3),
\end{aligned}
\tag{11a–f}
$$

where

$$
\begin{aligned}
\left(A_{ij}, B_{ij}, C_{ij}, D_{ij}, E_{ij}, F_{ij}\right) &= \int_{-h/2}^{h/2} Q_{ij(z)}^{(k)}(1, z, f(z), g(z), f'(z), g'(z))\mathrm{d}z,\\
(G_{ij}, H_{ij}, I_{ij}, J_{ij}, K'_{ij}) &= \int_{-h/2}^{h/2} Q_{ij(z)}^{(k)}(z^2, zf(z), zg(z), zf'(z), zg'(z))\mathrm{d}z,\\
(L_{ij}, M'_{ij}, N'_{ij}, O_{ij}) &= \int_{-h/2}^{h/2} Q_{ij(z)}^{(k)}(f^2(z), f(z)g(z), f(z)f'(z), f(z)g'(z))\mathrm{d}z,\\
(P'_{ij}, Q'_{ij}, R'_{ij}) &= \int_{-h/2}^{h/2} Q_{ij(z)}^{(k)}(g^2(z), g(z)f'(z), g(z)g'(z))\mathrm{d}z,\\
\left(S_{ij}, T_{ij}\right) &= \int_{-h/2}^{h/2} Q_{ij(z)}^{(k)}\left(f'^2(z), f'(z)g'(z)\right)\mathrm{d}z,\\
U_{ij} &= \int_{-h/2}^{h/2} Q_{ij(z)}^{(k)} g'^2(z)dz.
\end{aligned}
\tag{12a–f}
$$

From Eqs. (11a–f), it can be noticed that for N_i, M_i, P_i, Q_i, K_i, and R_i, the variables depending on x and y are the strains, $\varepsilon_j^b (b = 0, \ldots, 5)$. Therefore, the expressions in each of the plates governing equations (10a–d), for example, $\frac{\partial^2 M_i}{\partial x^2}$, can be expressed as follows:

$$
\begin{aligned}
\frac{\partial^2 M_i}{\partial x^2} = B_{ij} &\left[\begin{bmatrix}
\alpha^3 & 0 & 0 & 0\\
0 & \alpha^2\beta & 0 & 0\\
0 & 0 & 0 & 0\\
0 & 0 & 0 & -q^{**}\alpha^2\beta\\
0 & 0 & 0 & -q^{**}\alpha^3\\
-\alpha^2\beta & -\alpha^3 & 0 & 0
\end{bmatrix}\begin{bmatrix} U_{rs'}\\ V_{rs'}\\ W^b_{rs'}\\ W^s_{rs'}\end{bmatrix}\right] \times \begin{Bmatrix} SS\\ SS\\ SS\\ SC\\ CS\\ CC\end{Bmatrix}\\
+ G_{ij} &\left[\begin{bmatrix}
0 & 0 & y^{**}\alpha^4 & q^{**}\alpha^4\\
0 & 0 & y^{**}\alpha^2\beta^2 & q^{**}\alpha^2\beta^2\\
0 & 0 & 0 & 0\\
0 & 0 & 0 & 0\\
0 & 0 & 0 & 0\\
0 & 0 & -2y^{**}\alpha^3\beta & -2q^{**}\alpha^3\beta
\end{bmatrix}\begin{bmatrix} U_{rs'}\\ V_{rs'}\\ W^b_{rs'}\\ W^s_{rs'}\end{bmatrix}\right] \times \begin{Bmatrix} SS\\ SS\\ SS\\ SC\\ CS\\ CC\end{Bmatrix}\\
+ H_{ij} &\left[\begin{bmatrix}
0 & 0 & 0 & \alpha^4\\
0 & 0 & 0 & \alpha^2\beta^2\\
0 & 0 & 0 & 0\\
0 & 0 & 0 & 0\\
0 & 0 & 0 & 0\\
0 & 0 & 0 & -2\alpha^3\beta
\end{bmatrix}\begin{bmatrix} U_{rs'}\\ V_{rs'}\\ W^b_{rs'}\\ W^s_{rs'}\end{bmatrix}\right] \times \begin{Bmatrix} SS\\ SS\\ SS\\ SC\\ CS\\ CC\end{Bmatrix}
\end{aligned}
$$

$$
\begin{aligned}
&+I_{ij}\left[\begin{bmatrix}0&0&0&0\\0&0&0&0\\0&0&0&0\\0&0&0&-\alpha^2\beta\\0&0&0&-\alpha^3\\0&0&0&0\end{bmatrix}\begin{bmatrix}U_{rs'}\\V_{rs'}\\W^b_{rs'}\\W^s_{rs'}\end{bmatrix}\right]\times\begin{Bmatrix}SS\\SS\\SS\\SC\\CS\\CC\end{Bmatrix}\\
&+J_{ij}\left[\begin{bmatrix}0&0&0&0\\0&0&0&0\\0&0&0&0\\0&0&0&-\alpha^2\beta\\0&0&0&-\alpha^3\\0&0&0&0\end{bmatrix}\begin{bmatrix}U_{rs'}\\V_{rs'}\\W^b_{rs'}\\W^s_{rs'}\end{bmatrix}\right]\times\begin{Bmatrix}SS\\SS\\SS\\SC\\CS\\CC\end{Bmatrix}\\
&+K'_{ij}\left[\begin{bmatrix}0&0&0&0\\0&0&0&0\\0&0&0&-\alpha^2\\0&0&0&0\\0&0&0&0\\0&0&0&0\end{bmatrix}\begin{bmatrix}U_{rs'}\\V_{rs'}\\W^b_{rs'}\\W^s_{rs'}\end{bmatrix}\right]\times\begin{Bmatrix}SS\\SS\\SS\\SC\\CS\\CC\end{Bmatrix},
\end{aligned}
\tag{13}
$$

where $SS = \sin(\alpha x)\sin(\beta y)$, $SC = \sin(\alpha x)\cos(\beta y)$ and so on, and the elements of the 6×4 matrices are the coefficients obtained after taking the second derivation of the strains expression in Eqs. (11 a–f). As is known, the strains are expressed as a function of the four unknowns, described in Eqs. (1 a–c). These unknowns are expressed as shown in the Eqs. (17 a–d) in order to satisfy the simply supported boundary conditions.

The 6×4 matrices associated with $\frac{\partial^2 M_i}{\partial x^2}$ in Eq. (13) are called $\overline{M}_x^{2,b}(b = 0, \ldots, 5)$. The symbols used in $\overline{M}_v^{a,b}$ are as follows: the first upper and lower (a, v) indicate the derivative (second derivative with respect to x, in the example), and the second upper character, b, indicates that the derivative is associated with the strain $\varepsilon_j^b(b = 0, \ldots, 5)$. Therefore, the expression $\frac{\partial^2 M_i}{\partial x^2}$ can be expressed as

$$
\frac{\partial^2 M_i}{\partial x^2} = B_{ij}\overline{M}_x^{2,0} + G_{ij}\overline{M}_x^{2,1} + H_{ij}\overline{M}_x^{2,2} + I_{ij}\overline{M}_x^{2,3} + J_{ij}\overline{M}_x^{2,4} + K'_{ij}\overline{M}_x^{2,5},
\tag{14}
$$

where, for example, $\overline{M}_x^{2,0}$ is

$$
\overline{M}_x^{2,0} = \begin{bmatrix}\alpha^3 & 0 & 0 & 0\\ 0 & \alpha^2\beta & 0 & 0\\ 0 & 0 & 0 & 0\\ 0 & 0 & 0 & -q^{**}\alpha^2\beta\\ 0 & 0 & 0 & -q^{**}\alpha^3\\ -\alpha^2\beta & -\alpha^3 & 0 & 0\end{bmatrix}.
\tag{15}
$$

All matrices of type $\overline{M}_v^{a,b}$ associated with the expressions of the plate's governing equations (10 a–d), for example $\frac{\partial^2 M_i}{\partial x \partial y}$ or Q_i, are given in the "Appendix."

In what follows, the problem under consideration is solved for the following simply supported boundary conditions prescribed at all four edges:

$$
\begin{aligned}
N_1 = M_1 = P_1 = v = w_b = w_s = \frac{\partial w_s}{\partial y} \qquad &\text{at} \quad x = 0, a,\\
N_2 = M_2 = P_2 = u = w_b = w_s = \frac{\partial w_s}{\partial x} \qquad &\text{at} \quad y = 0, b.
\end{aligned}
\tag{16a–b}
$$

3 Solution procedure

Exact solutions of the partial differential equations (10a–d) on an arbitrary domain and for general boundary conditions are difficult. Although the Navier-type solutions can be used to validate the present theory, more general boundary conditions will require solution strategies involving, e.g., boundary discontinuous double Fourier series approach (see, for example, Oktem et al. [64]).

Solution functions that completely satisfy the boundary conditions in Eqs. (16a–b) are assumed as follows:

$$u(x,y) = \sum_{r=1}^{\infty}\sum_{s'=1}^{\infty} U_{rs'}\cos(\alpha x)\sin(\beta y), \quad 0 \le x \le a; \quad 0 \le y \le b, \tag{17a}$$

$$v(x,y) = \sum_{r=1}^{\infty}\sum_{s'=1}^{\infty} V_{rs'}\sin(\alpha x)\cos(\beta y), \quad 0 \le x \le a; \quad 0 \le y \le b, \tag{17b}$$

$$w_b(x,y) = \sum_{r=1}^{\infty}\sum_{s'=1}^{\infty} W^b_{rs'}\sin(\alpha x)\sin(\beta y), \quad 0 \le x \le a; \quad 0 \le y \le b, \tag{17c}$$

$$w_s(x,y) = \sum_{r=1}^{\infty}\sum_{s'=1}^{\infty} W^s_{rs'}\sin(\alpha x)\sin(\beta y), \quad 0 \le x \le a; \quad 0 \le y \le b, \tag{17d}$$

where

$$\alpha = \frac{r\pi}{a}, \quad \beta = \frac{s'\pi}{b}. \tag{18}$$

Substituting Eqs. (17a–d) into Eqs. (10a–d), the following equations are obtained:

$$K_{ij}d_j = F_j \quad (i,j = 1,\ldots,4) \text{ and } (K_{ij} = K_{ji}). \tag{19a}$$

Elements of K_{ij} in Eq. (19a) can be obtained by using the matrices $\overline{M}^{a,b}_{v}$ and the governing equations 10(a–d):

$$\{d_j\}^T = \left\{U_{rs}{}' \quad V_{rs'} \quad W^b_{rs'} \quad W^s_{rs'}\right\}, \tag{19b}$$

$$\{F_j\}^T = \left\{0 \quad 0 \quad Q_{rs'} - q^* \quad Q_{rs'}\right\}, \tag{19c}$$

where $Q_{rs'}$ are the coefficients in the double Fourier expansion of the transverse load. Note that with $-q^*Q_{rs}$, it is specified the position through the thickness where the load is applied, i.e., at the top or bottom of the plate in this case; see Eq. 1c and the last term in Eq. 7 to understand its vector position in Eq. 19c.

$$q(x,y) = \sum_{r=1}^{\infty}\sum_{s'=1}^{\infty} Q_{rs'}\sin(\alpha x)\sin(\beta y). \tag{20}$$

4 Numerical results and discussion

The bending analysis of FGPs is presented in this section. The selection of the parameters m and n of the shear strain shape functions described in Eqs. (1a–c) was performed considering several aspects: (a) first of all, the shear strain function should be expressed as a function of m and n (see Eqs. (1a–c)); (b) then, the strains and stresses will be also $f(z)$, $g(z)$, m, and n parameter-dependent; (c) consequently, the governing equations will be also m and n parameter-dependent; (d) by changing properly these parameters and running the bending problem thousands of times, output matrices containing displacements and stresses as a functions of m and n (see, for example, Fig. 4 for the non-dimensionalized vertical displacement at $(a/2, b/2, 0)$ and shear stresses at $(0, b/2, 0)$ as the function of the parameters m and n for the case problem studied in [22]) can be obtained at specific position of the plate (preferred at $z = 0$); (e) a simple MATLAB code, which uses the matrices obtained in (d), was coded in order to optimize and properly select the appropriated values of m and n, which produce a minimal error threshold with the 3D solutions [22] (case problem 1) and quasi-3D exact solution

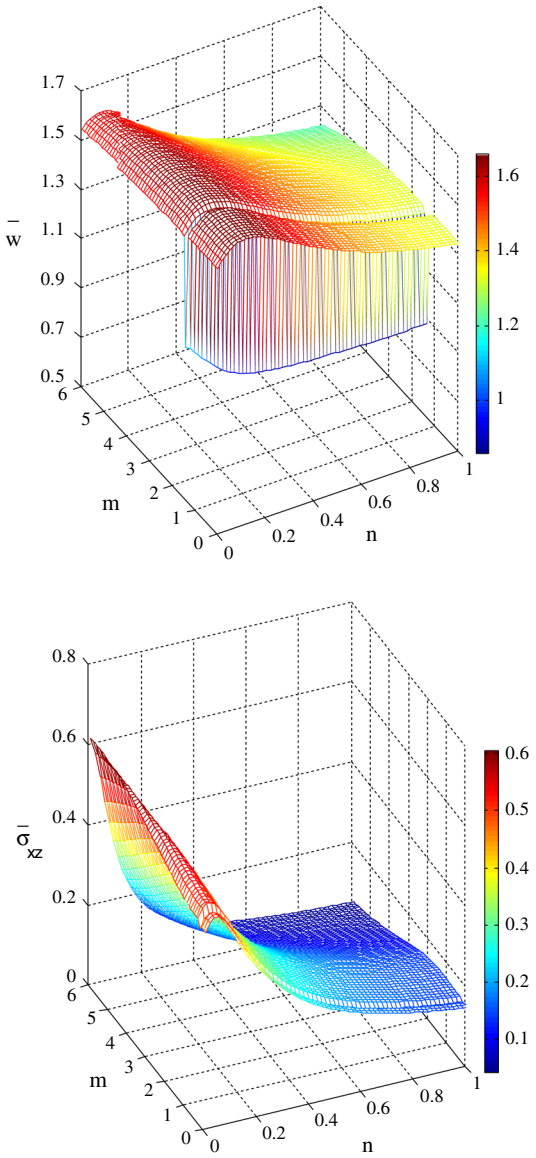

Fig. 4 Variations of non-dimensionalized vertical deflection ($a/b = 1/6$, $a/h = 2$ and $p = 1.5$) and transverse shear stresses ($a/b = 1/4$, $a/h = 4$ and $p = 0.5$) with parameters m and n

[43] (case problem 2); (f) finally, the selected values of m and n were used for validations, i.e., the distribution of displacement and stresses thought the plate thickness was compared again with the 3D solution [22] and not just in one point in the plate as in (d).

By following the above-mentioned steps, finally, the values for m and n are 1 and $\frac{3}{20}$, respectively.

In the next section, FGPs with elastic properties varying exponentially in z, as given by Zenkour [22] and FGPs with elastic properties powerly graded along the thickness direction z, as proposed by Zenkour [20] and accurately solved by Carrera et al. [43], are utilized to validate the present theory.

4.1 Case problem 1 (exponentially graded plates)

The bending analysis of this FGM is conducted by using aluminum (bottom, Al) graded exponentially trough the thickness of a rectangular plate (see Fig. 1a). The material properties used for computing the numerical results are

$$E_b = 70\,\text{GPa}, \quad v_b = 0.3. \tag{21}$$

Table 1 Non-dimensionalized center deflection $\overline{w}(a/2, b/2, 0)$ for various EGPs, $a/h = 2$

a/h	b/a	Theory	$p = 0.1$	$p = 0.5$	$p = 1.0$	$p = 1.5$
2	6	3-D [22]	1.638	1.352	1.059	0.826
		Present	1.657	1.352	1.043	0.800
		Ref. [55]	1.637	1.336	1.033	0.794
		Ref. [53]	1.735	1.418	1.100	0.850
		TPT [22]	1.629	1.331	1.028	0.791
		HSDT [22]	1.548	1.265	0.980	0.756
	1	3-D [22]	0.577	0.477	0.373	0.289
		Present	0.598	0.488	0.375	0.287
		Ref. [55]	0.578	0.472	0.365	0.279
		Ref. [53]	0.636	0.519	0.402	0.308
		TPT [22]	0.573	0.468	0.361	0.277
		HSDT [22]	0.586	0.478	0.369	0.282

Table 2 Non-dimensionalized normal stresses $\overline{\sigma}_{yy}(a/2, b/2, h/2)$ for various EGPs, $a/h = 4$

a/h	b/a	Theory	$p = 0.1$	$p = 0.5$	$p = 1.0$	$p = 1.5$
4	6	3-D [22]	0.218	0.247	0.289	0.337
		Present	0.197	0.220	0.253	0.294
		Ref. [55]	0.213	0.239	0.280	0.329
		Ref. [53]	0.201	0.230	0.271	0.319
		TPT [22]	0.237	0.268	0.314	0.370
		HSDT [22]	0.282	0.322	0.380	0.448
	1	3-D [22]	0.225	0.256	0.302	0.359
		Present	0.213	0.242	0.284	0.332
		Ref. [55]	0.224	0.255	0.301	0.356
		Ref. [53]	0.216	0.248	0.293	0.345
		TPT [22]	0.235	0.268	0.317	0.374
		HSDT [22]	0.241	0.276	0.326	0.385

Table 3 Non-dimensionalized center deflection $\overline{w}(a/2, b/2, 0)$ for various EGPs, $a/h = 10$

b/a	Theory	$p = 0.1$	$p = 0.5$	$p = 1.0$	$p = 1.5$	$p = 2.0$	$p = 2.5$	$p = 3.0$
6	Present	1.033	0.845	0.655	0.506	0.391	0.302	0.232
	Ref. [55]	1.035	0.846	0.656	0.507	0.391	0.302	0.232
	Ref. [53]	1.039	0.852	0.667	0.524	0.412	0.323	0.254
	TPT [55]	1.032	0.844	0.654	0.505	0.390	0.301	0.231
1	Present	0.279	0.228	0.177	0.137	0.106	0.081	0.063
	Ref. [55]	0.280	0.229	0.177	0.137	0.106	0.081	0.063
	Ref. [53]	0.282	0.231	0.181	0.142	0.111	0.087	0.068
	TPT [55]	0.279	0.228	0.177	0.137	0.105	0.081	0.062

The following formulas are utilized to normalize deflections and stresses:

$$\overline{w} = w\left(\frac{a}{2}, \frac{b}{2}, z\right)\frac{10E_b h^3}{q_0 a^4}, \quad \overline{\sigma}_{xx} = \sigma_{xx}\left(\frac{a}{2}, \frac{b}{2}, z\right)\frac{h^2}{q_0 a^2},$$
$$\overline{\sigma}_{yy} = \sigma_{yy}\left(\frac{a}{2}, \frac{b}{2}, z\right)\frac{h^2}{q_0 a^2}, \quad \overline{\sigma}_{xz} = \sigma_{xz}\left(0, \frac{b}{2}, z\right)\frac{h}{q_0 a}, \quad \overline{z} = \frac{z}{h}. \tag{22a–d}$$

As stated above, the bending results of this example problem are compared with the 3D exact solutions and the six-unknown TPTs with stretching effect by Zenkour [22]; and the quasi-3D HSDT with six unknowns by Mantari and Guedes Soares [55].

Results of non-dimensionalized vertical maximum displacement, normal stresses, and shears stresses are presented in Tables 1, 2, 3, 4, and 5. Results are in good agreement with the published results. Figure 5 shows the non-dimenzionalized distribution of vertical maximum deflection through the plate thickness ($b/a = \{1, 2, 3, 4\}$, $a/h = 4$, $p = 0.1$). Both closed-form solutions predict well the no-constant distribution of the central deflection (see Tables 1, 3 for more details). In Fig. 6, the non-dimensionalized normal stresses, $\overline{\sigma}_{xx}$,

Table 4 Non-dimensionalized normal stresses $\overline{\sigma}_{yy}(a/2, b/2, h/2)$ for various EGPs, $a/h = 10$

b/a	Theory	$p = 0.1$	$p = 0.5$	$p = 1.0$	$p = 1.5$	$p = 2.0$	$p = 2.5$	$p = 3.0$
6	Present	0.584	0.665	0.783	0.921	1.083	1.274	1.497
	Ref. [55]	0.601	0.686	0.808	0.951	1.118	1.312	1.539
	Ref. [53]	0.603	0.688	0.811	0.954	1.120	1.315	1.542
	TPT [55]	0.627	0.717	0.845	0.993	1.165	1.364	1.593
1	Present	0.198	0.224	0.263	0.309	0.363	0.428	0.506
	Ref. [55]	0.206	0.234	0.275	0.324	0.382	0.451	0.532
	Ref. [53]	0.206	0.235	0.277	0.326	0.384	0.450	0.528
	TPT [55]	0.220	0.250	0.294	0.346	0.407	0.477	0.560

Table 5 Non-dimensionalized shear stresses $\overline{\sigma}_{xz}(0, b/2, 0)$ for various EGPs, $a/h = 10$

b/a	Theory	$p = 0.1$	$p = 0.5$	$p = 1.0$	$p = 1.5$	$p = 2.0$	$p = 2.5$	$p = 3.0$
6	Present	0.492	0.484	0.460	0.425	0.382	0.336	0.291
	Ref. [55]	0.463	0.461	0.454	0.442	0.425	0.407	0.384
	Ref. [53]	0.463	0.461	0.454	0.441	0.425	0.406	0.384
	TPT [55]	0.478	0.475	0.468	0.456	0.440	0.421	0.398
1	Present	0.246	0.242	0.232	0.215	0.195	0.173	0.151
	Ref. [55]	0.238	0.237	0.233	0.227	0.218	0.209	0.199
	Ref. [53]	0.238	0.237	0.233	0.227	0.218	0.209	0.198
	TPT [55]	0.245	0.244	0.240	0.234	0.226	0.216	0.204

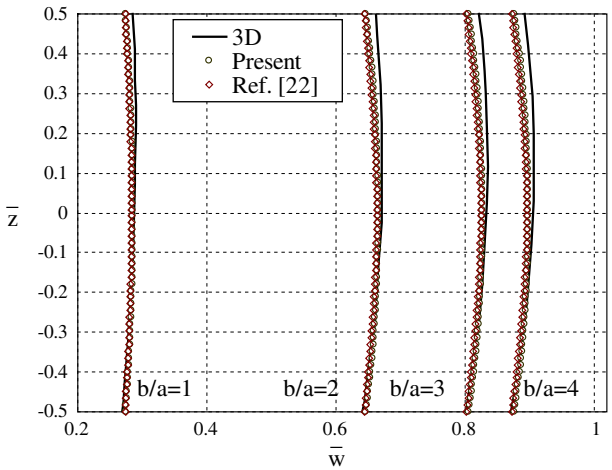

Fig. 5 Distribution of non-dimensionalized displacement, $\overline{w}(a/2, b/2, z)$, through the thickness of a thick EGP ($a/h = 4$ and $p = 0.5$)

through the plate thickness are shown. As in the vertical deflection, good results are achieved for both closed-form solutions (see Tables 2, 4 for more normal stresses results). In Fig. 7, the non-dimensionalized shear stresses, $\overline{\sigma}_{xz}$, distribution through the plate thickness, are shown. The present theory produces good results compared with 3D solution and as good as the TPT with six unknowns developed by Zenkour [22]. Therefore, this theory needs further research from the analytical and numerical point of view.

4.2 Case problem 2 (powerly graded plates)

A square FGP made of metal and ceramic powerly graded through its thickness is shown in Fig. 1b. The Young's modulus varies in thickness direction according to Eq. (4b), see also Fig. 3:

$$E_b = 70 \quad \text{GPa}, \quad E_t = 380 \quad \text{Gpa}, \quad v_b = v_t = 0.3. \tag{23}$$

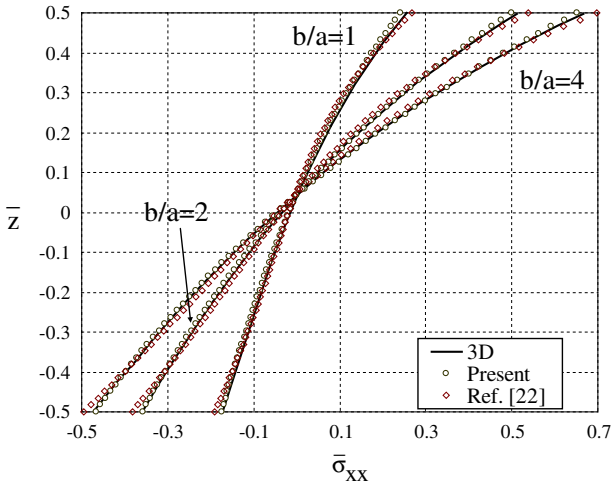

Fig. 6 Distribution of non-dimensionalized normal stress, $\overline{\sigma}_{xx}(a/2, b/2, z)$, through the thickness of a thick EGP ($a/h = 4$ and $p = 0.5$)

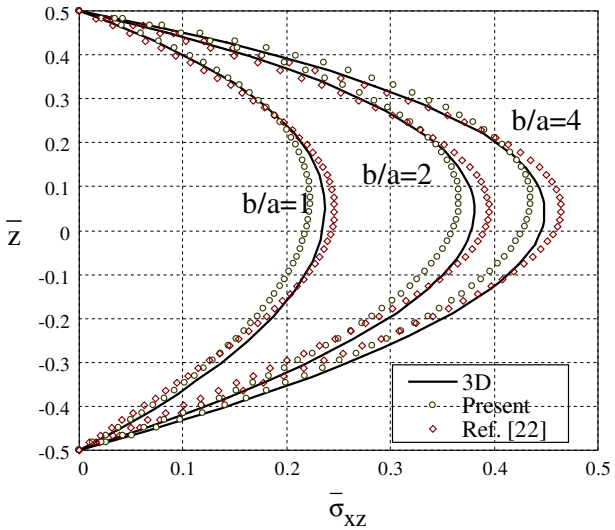

Fig. 7 Distribution of non-dimensionalized shear stress, $\overline{\sigma}_{xz}(0, b/2, z)$, through the thickness of a thick EGP ($a/h = 4$ and $p = 0.5$)

The following non-dimensional quantities are used:

$$\begin{aligned}
&\overline{u}(z) = \frac{100h^3E_t}{qa^4}u\left(0, \frac{b}{2}, z\right), \quad \overline{w}(z) = \frac{10h^3E_t}{qa^4}w\left(\frac{a}{2}, \frac{b}{2}, z\right),\\
&\overline{\sigma}_{xx}(z) = \sigma_{xx}\frac{h}{qa}\left(\frac{a}{2}, \frac{b}{2}, z\right), \quad \overline{\sigma}_{yy}(z) = \sigma_{yy}\frac{h}{qa}\left(\frac{a}{2}, \frac{b}{2}, z\right),\\
&\overline{\sigma}_{xy}(z) = \sigma_{xy}\frac{h}{qa}(0, 0, z), \quad \overline{\sigma}_{yz}(z) = \sigma_{yz}\frac{h}{qa}\left(\frac{a}{2}, 0, z\right),\\
&\overline{\sigma}_{xz}(z) = \sigma_{xz}\frac{h}{qa}\left(0, \frac{b}{2}, z\right)
\end{aligned} \tag{24a–g}$$

There exist accurate referential results [43] for this example problem. This paper considers it for validation. The reference solution was obtained by means of a discrete model, as described in [43]. Table 6 presents solutions from the CPT and FSDT, and quasi-3D HSDT [42,47] with a higher number of unknowns than in

Table 6 Non-dimensionalized deflection and shear stress of square PGPs, $a/h = 10$

p	Theory	$(a/2, b/2, 0)$			$(a/2, b/2, h/3)$		
		$a/h = 4$	$a/h = 10$	$a/h = 100$	$a/h = 4$	$a/h = 10$	$a/h = 100$
1	Ref. [43]	0.717	0.588	0.563	0.622	1.506	14.969
	Present	0.693	0.569	0.545	0.587	1.495	14.95
	Ref. [47]	0.7	0.585	0.562	0.593	1.495	14.969
	FSDT [42]	0.729	0.589	0.563	0.806	2.015	20.15
	CPT [42]	0.562	0.562	0.562	0.806	2.015	20.15
4	Ref. [43]	1.159	0.882	0.829	0.488	1.197	11.923
	Present	1.085	0.838	0.793	0.437	1.169	11.85
	Ref. [47]	1.118	0.875	0.829	0.44	1.178	11.932
	FSDT [42]	1.113	0.874	0.829	0.642	1.605	16.049
	CPT [42]	0.828	0.828	0.828	0.642	1.605	16.049
10	Ref. [43]	1.375	1.007	0.936	0.37	0.897	8.908
	Present	1.308	0.972	0.911	0.324	0.882	8.973
	Ref. [47]	1.349	0.875	0.829	0.323	1.178	11.932
	FSDT [42]	1.318	0.997	0.936	0.48	1.199	11.99
	CPT [42]	0.935	0.935	0.935	0.48	1.199	11.99

Table 7 Non-dimensionalized displacements and stresses of several square PGPs, $a/h = \{4, 10, 100\}$

p	Theory	$\overline{u}\left(-\frac{h}{4}\right)$	$\overline{u}\left(-\frac{h}{6}\right)$	$\overline{w}(0)$	$\overline{\sigma}_{xx}\left(\frac{h}{2}\right)$	$\overline{\sigma}_{yy}\left(\frac{h}{3}\right)$	$\overline{\sigma}_{yz}\left(\frac{h}{6}\right)$	$\overline{\sigma}_{xz}(0)$	$\overline{\sigma}_{xy}\left(-\frac{h}{3}\right)$
1	Present	0.587	0.446	0.569	2.931	1.495	0.274	0.246	0.564
	Ref. [20]	0.663	0.509	0.589	3.087	1.489	0.262	0.246	0.611
2	Present	0.812	0.633	0.722	3.409	1.389	0.249	0.196	0.496
	Ref. [20]	0.928	0.731	0.757	3.609	1.395	0.276	0.227	0.544
3	Present	0.911	0.714	0.796	3.634	1.264	0.217	0.161	0.505
	Ref. [20]	1.045	0.827	0.838	3.874	1.275	0.272	0.211	0.553
5	Present	0.974	0.759	0.868	3.955	1.096	0.171	0.136	0.530
	Ref. [20]	1.116	0.879	0.912	4.249	1.103	0.243	0.202	0.576
10	Present	1.002	0.762	0.972	4.743	0.882	0.140	0.145	0.554
	Ref. [20]	1.137	0.876	1.009	5.089	0.878	0.204	0.220	0.589

the theory presented here. The exponent that specifies the material variation profile through the thickness and side-to-thickness ratio are $p = \{1, 4, 10\}$ and $a/h = \{4, 10, 100\}$, respectively.

Table 7 presents non-dimensionalized displacements ($\overline{u}$ and $\overline{w}$) and normal, in-plane shear, and transverse shear stresses ($\overline{\sigma}_{xx}$, $\overline{\sigma}_{yy}$, $\overline{\sigma}_{xy}$, $\overline{\sigma}_{xz}$, and $\overline{\sigma}_{yz}$) for simply supported homogenous square plate subjected to bi-sinusoidal distributed load. The considered exponent and side-to-thickness ratio are $p = \{1, 2, 3, 5, 10\}$ and $a/h = 10$, respectively. Good results as in Zenkour [20] ($\varepsilon_{zz} = 0$) are achieved by the present theory. However, as p increases, the shear stresses results lost accuracy ($p \geq 5$). This may be perhaps alleviated when a refined hybrid-type shear strain shape function is utilized to model the displacement field ($g(z) \neq nf'(z)$).

From a general overview, it can be concluded that due to the accuracy of the present theory and its reduced number of unknowns, this paper delivers a new type of quasi-3D shear deformation theory not available in the literature with potential for further investigation due to the reduced number of unknowns.

5 Conclusions

An unavailable trigonometric quasi-3D HSDT with only four unknowns and stretching effects is presented in this paper. The governing equations and boundary conditions are derived by employing the principle of virtual work. Results show that the present theory is capable to produce very accurate results compared with other quasi-3D HSDTs with higher number of unknowns and so deserves special attention and further implementation by using numerical methods.

Acknowledgments The first author has been financed by the Portuguese Foundation of Science and Technology under the contract number SFRH/BPD/91210/2012.

Appendix: Definition of the matrices of type $\overline{M}_v^{a,b}$

As mentioned before, these matrices are associated with the expressions of the plate

$$\overline{M}^{0,0} = \begin{bmatrix} -\alpha & 0 & 0 & 0 \\ 0 & -\beta & 0 & 0 \\ 0 & 0 & 0 & 0 \\ 0 & 0 & 0 & q^{**}\beta \\ 0 & 0 & 0 & q^{**}\alpha \\ \beta & \alpha & 0 & 0 \end{bmatrix}, \quad \overline{M}^{0,1} = \begin{bmatrix} 0 & 0 & -y^{**}\alpha^2 & -q^{**}\alpha^2 \\ 0 & 0 & -y^{**}\beta^2 & -q^{**}\beta^2 \\ 0 & 0 & 0 & 0 \\ 0 & 0 & 0 & 0 \\ 0 & 0 & 0 & 0 \\ 0 & 0 & 2y^{**}\alpha\beta & 2q^{**}\alpha\beta \end{bmatrix},$$

$$\overline{M}^{0,2} = \begin{bmatrix} 0 & 0 & 0 & -\alpha^2 \\ 0 & 0 & 0 & -\beta^2 \\ 0 & 0 & 0 & 0 \\ 0 & 0 & 0 & 0 \\ 0 & 0 & 0 & 0 \\ 0 & 0 & 0 & 2\alpha\beta \end{bmatrix}, \quad \overline{M}^{0,3} = \begin{bmatrix} 0 & 0 & 0 & 0 \\ 0 & 0 & 0 & 0 \\ 0 & 0 & 0 & 0 \\ 0 & 0 & 0 & \beta \\ 0 & 0 & 0 & \alpha \\ 0 & 0 & 0 & 0 \end{bmatrix},$$

$$\overline{M}^{0,4} = \begin{bmatrix} 0 & 0 & 0 & 0 \\ 0 & 0 & 0 & 0 \\ 0 & 0 & 0 & 0 \\ 0 & 0 & 0 & \beta \\ 0 & 0 & 0 & \alpha \\ 0 & 0 & 0 & 0 \end{bmatrix}, \quad \overline{M}^{0,5} = \begin{bmatrix} 0 & 0 & 0 & 0 \\ 0 & 0 & 0 & 0 \\ 0 & 0 & 0 & 1 \\ 0 & 0 & 0 & 0 \\ 0 & 0 & 0 & 0 \\ 0 & 0 & 0 & 0 \end{bmatrix},$$

$$\overline{M}_x^{1,0} = \begin{bmatrix} -\alpha^2 & 0 & 0 & 0 \\ 0 & -\alpha\beta & 0 & 0 \\ 0 & 0 & 0 & 0 \\ 0 & 0 & 0 & q^{**}\alpha\beta \\ 0 & 0 & 0 & -q^{**}\alpha^2 \\ -\alpha\beta & -\alpha^2 & 0 & 0 \end{bmatrix}, \quad \overline{M}_x^{1,1} = \begin{bmatrix} 0 & 0 & -y^{**}\alpha^3 & -q^{**}\alpha^3 \\ 0 & 0 & -y^{**}\alpha\beta^2 & -q^{**}\alpha\beta^2 \\ 0 & 0 & 0 & 0 \\ 0 & 0 & 0 & 0 \\ 0 & 0 & 0 & 0 \\ 0 & 0 & 2y^{**}\alpha^2\beta & 2q^{**}\alpha^2\beta \end{bmatrix},$$

$$\overline{M}_x^{1,2} = \begin{bmatrix} 0 & 0 & 0 & -\alpha^3 \\ 0 & 0 & 0 & -\alpha\beta^2 \\ 0 & 0 & 0 & 0 \\ 0 & 0 & 0 & 0 \\ 0 & 0 & 0 & 0 \\ 0 & 0 & 0 & 2\alpha^2\beta \end{bmatrix}, \quad \overline{M}_x^{1,3} = \begin{bmatrix} 0 & 0 & 0 & 0 \\ 0 & 0 & 0 & 0 \\ 0 & 0 & 0 & 0 \\ 0 & 0 & 0 & \alpha\beta \\ 0 & 0 & 0 & -\alpha^2 \\ 0 & 0 & 0 & 0 \end{bmatrix}, \quad \overline{M}_y^{1,4} = \begin{bmatrix} 0 & 0 & 0 & 0 \\ 0 & 0 & 0 & 0 \\ 0 & 0 & 0 & 0 \\ 0 & 0 & 0 & \alpha\beta \\ 0 & 0 & 0 & -\alpha^2 \\ 0 & 0 & 0 & 0 \end{bmatrix},$$

$$\overline{M}_x^{1,5} = \begin{bmatrix} 0 & 0 & 0 & 0 \\ 0 & 0 & 0 & 0 \\ 0 & 0 & 0 & \alpha \\ 0 & 0 & 0 & 0 \\ 0 & 0 & 0 & 0 \\ 0 & 0 & 0 & 0 \end{bmatrix},$$

$$\overline{M}_y^{1,0} = \begin{bmatrix} -\alpha\beta & 0 & 0 & 0 \\ 0 & -\beta^2 & 0 & 0 \\ 0 & 0 & 0 & 0 \\ 0 & 0 & 0 & -q^{**}\beta^2 \\ 0 & 0 & 0 & q^{**}\alpha\beta \\ -\beta^2 & -\alpha\beta & 0 & 0 \end{bmatrix}, \overline{M}_y^{1,1} = \begin{bmatrix} 0 & 0 & -y^{**}\alpha^2\beta & -q^{**}\alpha^2\beta \\ 0 & 0 & -y^{**}\beta^3 & -q^{**}\beta^3 \\ 0 & 0 & 0 & 0 \\ 0 & 0 & 0 & 0 \\ 0 & 0 & 0 & 0 \\ 0 & 0 & -2y^{**}\alpha\beta^2 & -2q^{**}\alpha\beta^2 \end{bmatrix},$$

$$\overline{M}_y^{1,2}=\begin{bmatrix}0&0&0&-\alpha^2\beta\\0&0&0&-\beta^3\\0&0&0&0\\0&0&0&0\\0&0&0&0\\0&0&0&-2\alpha\beta^2\end{bmatrix},\ \overline{M}_y^{1,3}=\begin{bmatrix}0&0&0&0\\0&0&0&0\\0&0&0&0\\0&0&0&-\beta^2\\0&0&0&\alpha\beta\\0&0&0&0\end{bmatrix},\ \overline{M}_y^{1,4}=\begin{bmatrix}0&0&0&0\\0&0&0&0\\0&0&0&0\\0&0&0&-\beta^2\\0&0&0&\alpha\beta\\0&0&0&0\end{bmatrix},$$

$$\overline{M}_y^{1,5}=\begin{bmatrix}0&0&0&0\\0&0&0&0\\0&0&0&\beta\\0&0&0&0\\0&0&0&0\\0&0&0&0\end{bmatrix},$$

$$\overline{M}_{xy}^{2,0}=\begin{bmatrix}-\alpha^2\beta&0&0&0\\0&-\alpha\beta^2&0&0\\0&0&0&0\\0&0&0&-q^{**}\alpha\beta^2\\0&0&0&-q^{**}\alpha^2\beta\\\beta&\alpha&0&0\end{bmatrix},\quad \overline{M}_{xy}^{2,1}=\begin{bmatrix}0&0&-y^{**}\alpha^3\beta&-q^{**}\alpha^3\beta\\0&0&-y^{**}\alpha\beta^3&-q^{**}\alpha\beta^3\\0&0&0&0\\0&0&0&0\\0&0&0&0\\0&0&2y^{**}\alpha^2\beta^2&2q^{**}\alpha^2\beta^2\end{bmatrix},$$

$$\overline{M}_{xy}^{2,2}=\begin{bmatrix}0&0&0&-\alpha^3\beta\\0&0&0&-\alpha\beta^3\\0&0&0&0\\0&0&0&0\\0&0&0&0\\0&0&0&2\alpha^2\beta^2\end{bmatrix},\quad \overline{M}_{xy}^{2,3}=\begin{bmatrix}0&0&0&0\\0&0&0&0\\0&0&0&0\\0&0&0&-\alpha\beta^2\\0&0&0&-\alpha^2\beta\\0&0&0&0\end{bmatrix},\quad \overline{M}_{xy}^{2,4}=\begin{bmatrix}0&0&0&0\\0&0&0&0\\0&0&0&0\\0&0&0&-\alpha\beta^2\\0&0&0&-\alpha^2\beta\\0&0&0&0\end{bmatrix},$$

$$\overline{M}_{xy}^{2,5}=\begin{bmatrix}0&0&0&0\\0&0&0&0\\0&0&0&\alpha\beta\\0&0&0&0\\0&0&0&0\\0&0&0&0\end{bmatrix}.$$

References

1. Bever, M.B., Duwez, P.E.: Gradients in composite materials. Mater. Sci. Eng. **10**, 1–8 (1972)
2. Koizumi, M.: The concept of FGM. Ceramic transactions. Funct. Grad. Mater. **34**, 3–10 (1993)
3. Jha, D.K., Kant, T., Singh, R.K.: A critical review of recent research on functionally graded plates. Compos. Struct. **96**, 833–849 (2013)
4. Birman, V., Byrd, L.W.: Modeling and analysis of functionally graded materials and structures. ASME Appl. Mech. Rev. **60**, 195–216 (2007)
5. Demasi, L.: ∞^6 Mixed plate theories based on the generalized unified formulation. Part I: governing equations. Compos. Struct. **87**, 1–11 (2009)
6. Demasi, L.: ∞^6 Mixed plate theories based on the generalized unified formulation. Part II: layerwise theories. Compos. Struct. **87**, 12–22 (2009)
7. Carrera, E.: An assessment of mixed and classical theories on global and local response of multilayered orthotropic plates. Compos. Struct. **50**, 183–198 (2000)
8. Carrera, E.: Developments, ideas, and evaluations based upon Reissner's mixed variational theorem in the modeling of multilayered plates and shells. Appl. Mech. Rev. **54**, 301–329 (2001)
9. Carrera, E.: Theories and finite elements for multilayered, anisotropic, composite plates and shells. Arch. Comput. Methods Eng. **9**(2), 87–140 (2002)
10. Demasi, L.: Treatment of stress variables in advanced multilayered plate elements based upon Reissners's mixed variational theorem. Compos. Struct. **84**, 1215–1221 (2006)
11. Demasi, L.: ∞^6 Mixed plate theories based on the generalized unified formulation. Part III: advanced mixed high order shear deformation theories. Compos. Struct. **87**, 183–194 (2009)

12. Demasi, L.: ∞^6 Mixed plate theories based on the generalized unified formulation. Part IV: zig–zag theories. Compos. Struct. **87**, 195–205 (2009)
13. Demasi, L.: ∞^6 Mixed plate theories based on the generalized unified formulation. Part V: results. Compos. Struct. **88**, 1–16 (2009)
14. Carrera, E.: Theories and finite elements for multilayered plates and shells: a unified compact formulation with numerical assessment and benchmarks. Arch. Comput. Methods Eng. **10**, 215–296 (2003)
15. Reddy, J.N.: Analysis of functionally graded plates. Int. J. Numer. Methods Eng. **47**, 663–684 (2000)
16. Cheng, Z.Q, Batra, R.C.: Deflection relationships between the homogeneous Kirchhoff plate theory and different functionally graded plate theories. Arch. Mech. **52**, 143–158 (2000)
17. Kashtalyan, M.: Three-dimensional elasticity solution for bending of functionally graded plates. Eur. J. Mech. A Solid **23**, 853–864 (2004)
18. Ferreira, A.J.M., Batra, R.C., Roque, C.M.C., Qian, L.F., Martins, P.A.L.S.: Static analysis of functionally graded plates using third-order shear deformation theory. Compos. Struct. **69**, 449–457 (2005)
19. Elishakoff, I.: Three-dimensional analysis of an all-round clamped plate made of functionally graded materials. Acta. Mech. **180**, 21–36 (2005)
20. Zenkour, A.M.: Generalized shear deformation theory for bending analysis of functionally graded plates. Appl. Math. Model. **30**, 67–84 (2006)
21. Ramirez, F., Heyliger, P.R., Pan, E.: Static analysis of functionally graded elastic Anisotropic plates using a discrete layer approach. Compos. Part B **37**, 10–20 (2006)
22. Zenkour, A.M.: Benchmark trigonometric and 3-D elasticity solutions for an exponentially graded thick rectangular plate. Appl. Math. Model. **77**, 197–214 (2007)
23. Sladek, J., Sladek, V., Hellmich, CH., Eberhardsteiner, J.: Analysis of thick functionally graded plates by local integral equation. Commun. Numer. Methods Eng. **23**, 733–754 (2007)
24. Sladek, J., Sladek, V., Solek, P., Wen, PH.: Thermal bending of Reissner–Mindlin plates by the MLPG, CMES. Comput. Model. Eng. Sci. **28**, 57–76 (2008)
25. Sladek, J., Sladek, V., Solek, P., Wen, P.H., Atluri, S.N.: Thermal analysis of Reissner–Mindlin shallow shells with FGM properties by the MLPG, CMES. Comput. Model. Eng. Sci. **30**, 77–97 (2008)
26. Abrate, S.: Functionally graded plates behave like homogeneous plates. Compos. Part B **39**, 151–158 (2008)
27. Bo, Y, Hao-Jiang, D., Wei-Qiu, C.: Elasticity solutions for functionally graded plates in cylindrical bending. Appl. Math. Mech. **29**(8), 999–1004 (2008)
28. Matsunaga, H.: Free vibration and stability of functionally graded plates according to 2-D higher-order deformation theory. Compos. Struct. **82**, 256–270 (2008)
29. Matsunaga, H.: Stress analysis of functionally graded plates subjected to thermal and mechanical loadings. Compos. Struct. **87**, 344–357 (2009)
30. Matsunaga, H.: Thermal buckling of functionally graded plates according to a 2D higher-order deformation theory. Compos. Struct. **90**, 76–86 (2009)
31. Khabbaz, R.S., Manshadi, B.D., Abedian, A.: Nonlinear analysis of FGM plates under pressure loads using the higher-order shear deformation theories. Compos. Struct. **89**, 333–344 (2009)
32. Aghdam, M.M., Bigdelli, K., Shahmansouri, N.: A semi-analytical solution for bending of moderately thick curved functionally graded panels. Mech. Adv. Mater. Struct. **17**, 320–327 (2010)
33. Zenkour, A.M., Alghamdi, N.A.: Thermomechanical bending response of functionally graded nonsymmetric sandwich plates. J. Sandw. Struct. Mater. **12**, 7–46 (2010)
34. Wu, C.P., Li, H.Y.: An RMVT-based third-order shear deformation theory of multilayered functionally graded material plates. Compos. Struct. **92**, 2591–2605 (2010)
35. Talha, M., Singh, B.N.: Static response and free vibration analysis of FGM plates using higher order shear deformation theory. Appl. Math. Model. **34**, 3991–4011 (2010)
36. Vaghefi, R., Baradaran, G.H., Koohkan, H.: Three-dimensional static analysis of thick functionally graded plates by using meshless local Petrov–Galerkin (MLPG) method. Eng. Anal. Bound. Elem. **34**, 564–573 (2010)
37. Wu, C.P., Chiu, K.H., Wang, Y.M.: RMVT-based meshless collocation and element free Galerkin methods for the quasi-3D analysis of multilayered composite and FGM plates. Compos. Struct. **93**, 923–943 (2011)
38. Wu, C.P., Yang, S.W.: RMVT-based meshless collocation and element-free Galerkin methods for the quasi-3D analysis of multilayered composite and FGM circular hollow cylinders. Compos. Part B **42**, 1683–1700 (2011)
39. Benachour, A., Tahar, H.D., Atmane, H.A., Tounsi, A., Ahmed, M.S.: A four variable refined plate theory for free vibrations of functionally graded plates with arbitrary gradient. Compos. Part B **42**, 1386–1394 (2011)
40. Thai, H.T., Choi, D.H.: A refined shear deformation theory for free vibration of functionally graded plates on elastic foundation. Compos. Part B **43**, 2335–2347 (2011)
41. Reddy, J.N., Kim, J.: A nonlinear modified couple stress-based third-order theory of functionally graded plates. Compos. Struct. **94**, 1128–1143 (2012)
42. Carrera, E., Brischetto, S., Cinefra, M., Soave, M.: Effects of thickness stretching in functionally graded plates and shells. Compos. Part B **42**, 123–133 (2011)
43. Carrera, E., Brischetto, S., Robaldo, A.: Variable kinematics model for the analysis of functionally graded material plates. J. AIAA **46**, 194–203 (2008)
44. Brischetto, S.: Classical and mixed advanced models for sandwich plates embedding functionally graded cores. J. Mech. Mater. Struct. **4**, 13–33 (2009)
45. Brischetto, S., Carrera, E.: Classical and mixed theories for bending analysis of functionally graded materials shells. In: Proceedings of APCOM'07 in Conjunction with EPMESC XI, Kyoto, Japan (2007)
46. Brischetto, S., Carrera, E.: Advanced mixed theories for bending analysis of functionally graded plates. Comput. Struct. **88**, 1474–1483 (2010)

47. Neves, A.M.A., Ferreira, A.J.M., Carrera, E., Roque, C.M.C., Cinefra, M., Jorge, R.M.N., Soares, C.M.M.: Bending of FGM plates by a sinusoidal plate formulation and collocation with radial basis functions. Mech. Res. Commun. **38**, 368–371 (2011)
48. Neves, A.M.A., Ferreira, A.J.M., Carrera, E., Roque, C.M.C., Cinefra, M., Jorge, R.M.N., Soares, C.M.M.: A quasi-3D sinusoidal shear deformation theory for the static and free vibration analysis of functionally graded plates. Compos. Part B **43**, 711 (2012)
49. Neves, A.M.A., Ferreira, A.J.M., Carrera, E., Cinefra, M., Roque, C.M.C., Jorge, R.M.N.: A quasi-3D hyperbolic shear deformation theory for the static and free vibration analysis of functionally graded plates. Compos. Struct. **94**(5), 1814–1825 (2012)
50. Neves, A.M.A., Ferreira, A.J.M., Carrera, E., Cinefra, M., Roque, C.M.C., Jorge, R.M.N.: Static, free vibration and buckling analysis of isotropic and sandwich functionally graded plates using a quasi-3D higher-order shear deformation theory and a meshless technique. Compos. B Eng. **44**(1), 657–674 (2013)
51. Ferreira, A.J.M., Carrera, E., Cinefra, M., Roque, C.M.C., Polit, O.: Analysis of laminated shells by a sinusoidal shear deformation theory and radial basis functions collocation, accounting for through-the-thickness deformations. Compos. Part B **42**, 1276–1284 (2011)
52. Mantari, J.L., Oktem, A.S., Guedes Soares, C.: Bending response of functionally graded plates by using a new higher order shear deformation theory. Compos. Struct. **94**, 714–723 (2012)
53. Mantari, J.L., Guedes Soares, C.: Bending analysis of thick exponentially graded plates using a new trigonometric higher order shear deformation theory. Compos. Struct. **94**, 1991–2000 (2012)
54. Mantari, J.L., Guedes Soares, C.: Finite element formulation of a generalized higher order shear deformation theory for advanced composite plates. Compos. Struct. **96**, 545–553 (2013)
55. Mantari, J.L., Guedes Soares, C.: A novel higher-order shear deformation theory with stretching effect for functionally graded plates. Compos. Part B **45**, 268–281 (2013)
56. Mantari, J.L., Guedes Soares, C.: Generalized hybrid quasi-3D shear deformation theory for the static analysis of advanced composite plates. Compos. Struct. **94**, 2561–2575 (2012)
57. Xiang, S., Kang, G.: A nth-order shear deformation theory for the bending analysis on the functionally graded plates. Eur. J. Mech. A Solids **37**, 336–343 (2013)
58. Mechab, B., Mechab, I., Benaissa, S.: Static and dynamic analysis of functionally graded plates using four-variable refined plate theory by the new function. Compos. Part B **45**, 748–757 (2013)
59. Thai, H.T., Kim, S.E.: A simple quasi-3D sinusoidal shear deformation theory for functionally graded plates. Compos. Struct. **99**, 172–180 (2013)
60. Mantari, J.L., Guedes Soares, C.: A Trigonometric Plate Theory with 5-Unknows and Stretching Effect for Advanced Composite Plates, Submitted for publication
61. Mantari, J.L., Guedes Soares, C.: Optimizing the Sinusoidal Higher Order Shear Deformation Theory, Submitted for publication
62. Zenkour, A.M.: A simple four-unknown refined theory for bending analysis of functionally graded plates. Appl. Math. Model. (2013). doi:10.1016/j.apm.2013.04.022
63. Reddy, J.N.: Mechanics of Laminated Composite Plates: Theory and Analysis, 2nd edn. CRC Press, Boca Raton, FL (2004)
64. Oktem, A.S., Mantari, J.L., Guedes Soares, C.: Static response of functionally graded plates and doubly-curved shells based on a higher order shear deformation theory. Eur. J. Mech. A Solids **36**, 163–172 (2012)